An experimental study of a combusting flow past a confined bluff body
Campbell, Ian; Logan, Douglas

AN EXPERIMENTAL STUDY OF A COMBUSTING FLOW PAST A CONFINED BLUFF BODY

I.G. Campbell and D.L. Logan
Combustion Research
Institute for Chemical Process and Environmental Technology
National Research Council of Canada
Ottawa, Ontario
K1A 0R6

Introduction

This paper presents an overview of the experimental results gathered during an extensive test program on a bluff body stabilized flame. While a variety of parameters were measured, the emphasis of this work was to investigate the distribution of soot and NO_x in the flame. Initial test of the facility indicated a change in the physical parameters at an equivalence ratio of approximately 0.5 to 0.6. From the observations a selection of two conditions ϕ=0.55 and 0.65, were used in the experimental program.

Experimental Apparatus

The combustion chamber, illustrated Figure 1, was a simple blowdown geometry. The stainless steel chamber measured 100 mm internal diameter, by 420 mm in length. A ceramic blanket covered the exterior of the chamber, except for the exit and instrumentation access points. A propane stream entered the chamber through the centre of a bluff body stabilizer. The stabilizer was centrally positioned in the air stream that passed into the chamber in a co-axial manner. Four quartz windows allowed measurements of axial and radial velocities using a 3 component LDA system. Substituting specially designed metal plates for the quartz windows allowed measurements of gas temperatures, radiation and major gas species through fixed axially located ports. The exit of the chamber was a 4:1 contraction nozzle. Replacing the aforementioned windowed chamber with a "pancake" version, not illustrated, allowed soot measurements using LII (Laser Induced Incandescence) techniques.

Gas species were measured using a water-cooled probe and a combination of gas chromatograph and NO_x analyser. The gas temperatures and radiation were measured using Pt/Pt-10%Rh thermocouples and radiometer respectively.

A further chamber substitution of a similarly dimension quartz tube, facilitated flow visualization using a laser sheet illumination to assist in understanding the fuel stream stability and dispersion in the wake of the bluff body.

Results and Discussion

Flow visualization of the fuel jet illustrated the dependence of the fuel stream stability on the ratio of fuel to air velocity ratio. Increasing the air to fuel velocity ratio beyond 1.7, resulted in a stable fuel dispersion coupled with a diminished centreline recirculation zone. Below this level, the fuel stream was in a continuously unsteady motion behind the bluff body. Examination of high-speed cine photographs for ϕ=0.65, the fuel stream was observed to intermittently penetrate the recirculation zone. The fuel penetration of the recirculation zone is observable in the measured mean axial flows of Figure 2. Along the centreline, the axial flow had a strong reversal for ϕ=0.55, but exhibited no reversal for ϕ=0.65. Plots of the axial velocity distribution, for ϕ=0.65, in this zone revealed that the flow had both a positive and negative component, but an overall positive mean value. For both cases the high air velocity entering the chamber around the bluff body can be seen at the axial and radial location of 10 and 30 mm respectively. The air flows outwardly towards the chamber wall with axial distance to approximately 50 mm before being drawn back towards the centreline forming the recirculation zone.

The gas temperatures for the two conditions, Figure 3, showed higher temperatures and wider bands for ϕ=0.65, than for ϕ=0.55. A peak temperature of 1720°C was recorded for ϕ=0.65, whereas 1670°C was the highest measured for the lower high equivalence ratio. While for the two conditions the temperatures contour plots are generally similar in shape, on the centreline the lower equivalence ratio attains a peak level before the high condition.

An example of the gas species measurements, Figure 4, showed that the CO_2 levels along the centreline varied due to the propane stream passing through the recirculation zone. The CO_2 levels produced at ϕ=0.55 are reached for ϕ=0.65 almost one chamber diameter further downstream. A suggested reason for the CO_2 shift on the centreline is due to the fuel passing through the recirculation zone. As the excess fuel reduces the air to fuel ratio at the end of the recirculation zone, there results a reduced CO_2 production until more air is entrained into that region. This same reason would also explain the quicker rise of temperatures for ϕ=0.55 than ϕ=0.65.

NO_x production was similar to that of CO_2. In the two cases the levels recorded, Figure 5, showed that the higher equivalence ratio produced more NO_x due to the higher temperatures down and across the upper section of the chamber. Separating the NO_x into NO and NO_2, showed NO production accounted for 75% of the recorded NO_x at most locations. The zone of NO_2 production differed from that of NO, by being in a zone closer to the chamber wall, were O_2 was more prevalent.

Radiation measurements at the inside surface of the chamber wall showed the expected increase in measured levels with higher axial locations in the chamber, Figure 6. At the higher equivalence ratio a peak radiation level was observed at three chamber diameters downstream of the nozzle, approximately 50% higher than for the other condition.

Preliminary results of the LII measurements (not shown here) indicated soot formation varied with the air to fuel velocity ratio. The soot formed at the equivalence ratio of 0.55 was observed to be under 1/10 that for ϕ=0.65. The number counts for both conditions showed soot formed one chamber diameter down stream of the bluff body and continued to form or grow to the last measuring section of the chamber. However, for ϕ=0.65, soot levels increased along the chamber, with axial distance. This observation was not seen for the ϕ=0.55 condition.

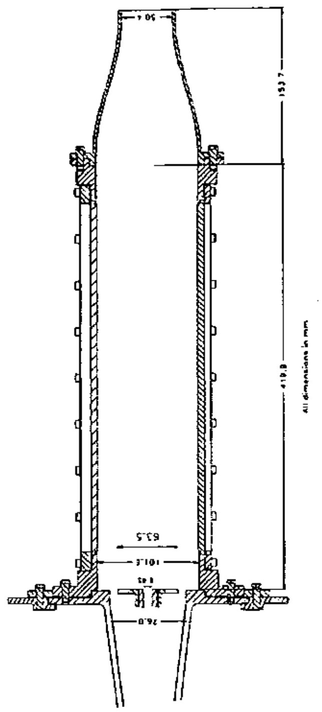

Figure 1 Combustion chamber

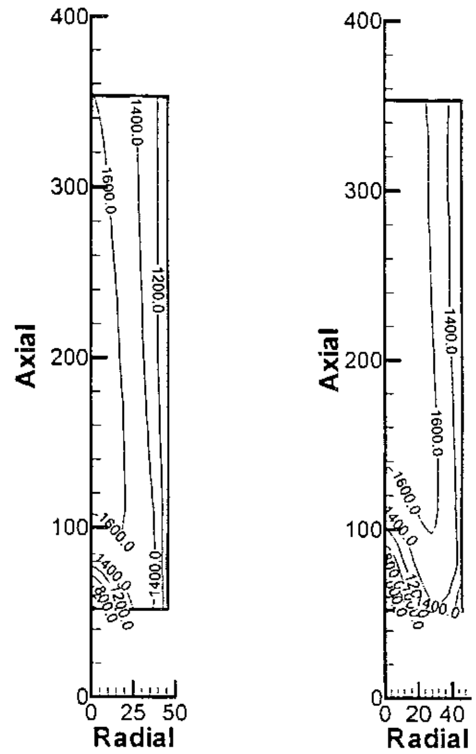

Figure 3 Gas temperatures (°C)

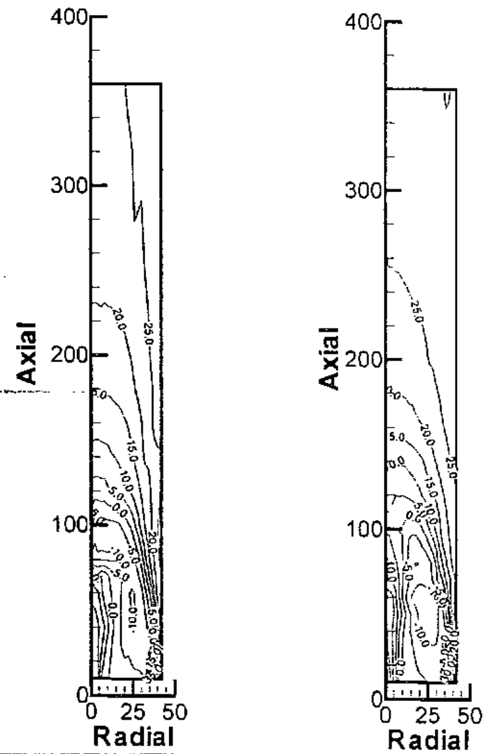

Figure 2 Mean axial velocity (m/s)

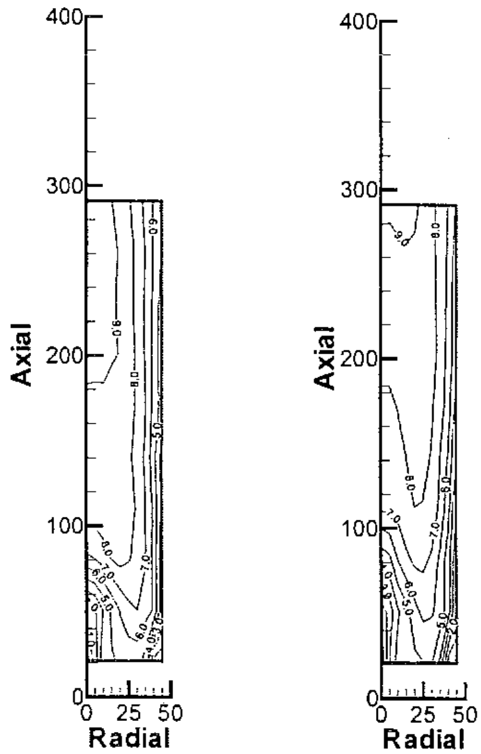

Figure 4 CO2 levels in chamber (% volume)

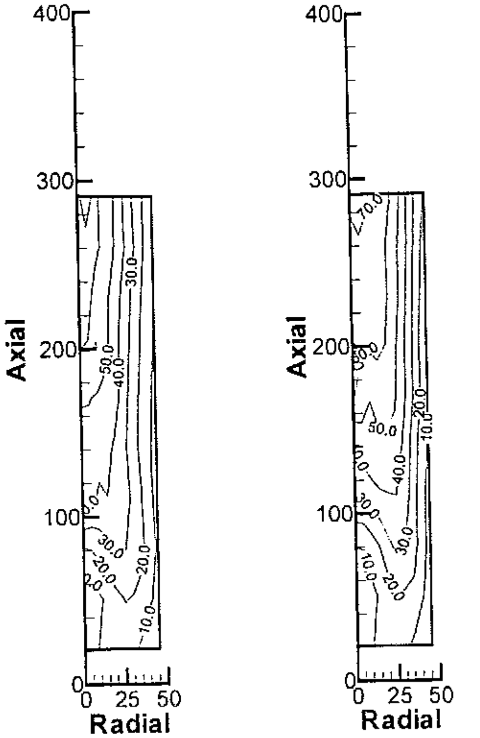

Figure 5 NOx levels in chamber (ppm)

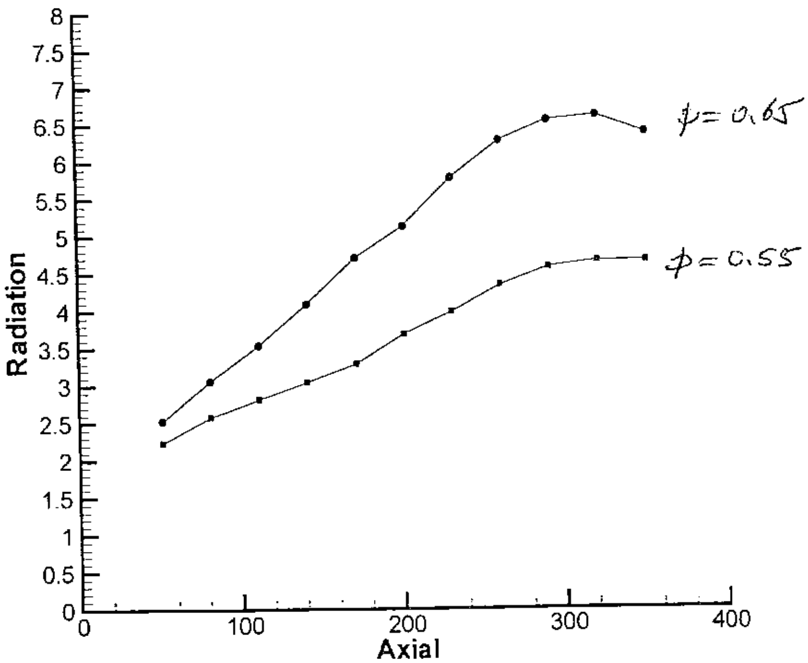

Figure 6 Radiation measurements (Btu/ft²s)

F. Liu

The Combustion Institute Canadian Section

1997 Spring Technical Meeting

25 to 28 May
DalTech
Halifax, NS